Journal of Optoelectronics and Advanced Materials Vol. 7, No. 3, June 2005, p. 1335 - 1340

INVESTIGATION ON THE STRUCTURAL AND OPTICAL PROPERTIES OF TIN OXIDE FILMS GROWN BY PULSED LASER DEPOSITION

T. J. Stanimirova*, P. A. Atanasov, I. G. Dimitrov, A. O. Dikovska

Institute of Electronics, Bulgarian Academy of Sciences, 72 Tsarigradsko Chausse Blvd., Sofia 1784, Bulgaria

Thin tin oxide (SnO_2) films have been grown on (001) SiO_2 substrate by pulsed laser deposition (PLD) technique. XeCl laser was used for ablation of SnO_2 ceramic targets at substrate temperatures ranging from room temperature to 500 °C and oxygen pressure in the range of 5 – 30 Pa. The structural and optical parameters of the layers have been studied as function of the deposition conditions. The oxygen pressure of 20 Pa was determined as an optimum one while the structural and optical properties vary with the substrate temperature. The film deposited at 500 °C and 20 Pa oxygen pressure has best crystalline properties, i.e. optimum growth conditions. However, film grown at 20 Pa and 200 °C has maximum transmission in the visible region. The refractive index of the film deposited at optimum growth conditions is 1.93, which is close to that of the bulk material (1.96). Moreover, film grown at 20 Pa and 400 °C has lowest (7 dB/cm) optical waveguide loss.

(Received April 12, 2005; accepted May 26, 2005)

Keywords: Tin oxide, PLD thin films, Optical properties

1. Introduction

Tin oxide (SnO_2) is an *n*-type semiconductor which possesses perfect physical properties, superior chemical stability and low cost. All these properties have stimulated its applications in active and passive electronic devices [1-3]. Additionally, the material shows high variations of the electrical resistance in the presence of oxidizing and reducing gases. Thin tin oxide films exhibit high optical transparency (> 80 %) in the visible region. These advantageous properties are used for gas sensor application [4,5]. The electrical gas sensors are sensitive to the electric or magnetic fields in contrast to the optical ones. Our main interest is focused on obtaining of thin tin oxide films, which would be appropriate for optical gas sensors.

There are many different techniques used for depositing tin oxide films: r. f. sputtering [6-13], dc-magnetron sputtering [14], thermal evaporation [15,16], ion beam deposition [17], rheotaxial growth and thermal oxidation (RGTO) [18-20], chemical vapour deposition [21-25], spray pyrolysis [26], successive ionic layer deposition (SILD) [27], and other chemical methods [28,29]. Sberveglieri [30] has presented a review of the techniques applied for tin oxide films deposition. As it is shown there, all methods discussed require high substrate temperature or post deposition annealing in order to fabricate good quality polycrystalline films. High temperature, however, damages the surface of the films and increases the interface thickness, which has negative effect on the optical properties, especially on the waveguiding.

Pulsed laser deposition technique was successfully applied for growing of quality thin tin oxide films [31-33]. They were produced by ablation of either Sn metal target [31] or SnO_2 target [33]. The substrate use were (100) Si, (001) SiO_2 [31] or Al_2O_3 [32,33].

We report on deposition of tin oxide layers on (001) SiO_2 substrate by laser ablation of SnO_2 ceramic targets. Silicon oxide is used as a substrate, because of its transparency and low refractive

* Corresponding author: t_stanimirova@yahoo.com

index, which is suitable for production of planar waveguide structures. The influence of the deposition conditions on the structural and optical properties of the produced layers was studied.

2. Experimental

The tin oxide thin films were produced in a standard PLD set-up. XeCl excimer laser (wavelength of 308 nm, pulse duration of 30 ns, and repetition rate of 2 Hz) was used for ablation of ceramic SnO_2 targets. All depositions were carried out at laser fluence of 1 $J.cm^{-2}$ in order to reduce the droplet formation.

The ceramics targets were prepared from SnO_2 (99.5 % purity) powder, which was pressed at 6 MPa to form pallets and then sintered at 1100 ^oC for 4 hours. The targets thus produced have high density and hardness.

The (001) SiO_2 plates having dimensions of 10×10 mm^2 were used as substrates in our experiments. They were cleaned in an ultrasonic bath before deposition. All substrates were located parallel to the target at a distance of 4 cm. The targets were rotated to ensure homogeneous erosion of its surface.

The chamber was evacuated down to 1×10^{-3} Pa. All depositions were performed in oxygen (99.99 % purity) pressure between 5 and 30 Pa. The deposition time was 90 min for all experiments. They were accomplished at substrate temperatures from the room temperature to 500 ^oC.

The crystalline structure of the films was analyzed by XRD measurements with CuKα radiation in θ - 2θ Bragg – Brentano geometry. A CARY-5E type spectrophotometer was used to obtain the optical transmission spectra in the wavelength range between 200 nm and 3000 nm. The refractive index and the thickness of the layers were determined by m - line spectroscopy using film – prism coupling. A $SrTiO_3$ prism was used to introduce He-Ne laser light into the films. The optical waveguide losses were measured by recording the attenuation of the scattered light along the propagation path.

3. Results and discussions

Films grown at oxygen pressure below 20 Pa are amorphous for all temperatures applied. At $P(O_2)$ = 20 Pa and higher, the films consist of SnO_{2-x} ($0 \leq x \leq 1$). The intensity of the peaks corresponding to SnO_2 phase has maximum values at 20 Pa, optimum oxygen pressure, and then decreases with the pressure raise. However, the intensity of the oxygen deficient phases has opposite trend.

The influence of deposition temperature on the films structure was investigated at $P(O_2)$ = 20 Pa. All the films grown at substrate temperature below 200 ^oC are amorphous. At T_s = 200 ^oC, the layer consists of amorphous phase mixed with oxygen deficient phases and shallow (110) SnO_2 crystallites. The amorphous phase completely disappears with further temperature increase and the films become polycrystalline with different SnO_{2-x} ($0 \leq x \leq 1$) phases. At 400 ^oC a transformation from SnO orthorhombic and Sn_2O_3 triclinic to SnO_2 tetragonal structure is observed. Furthermore, at 500 ^oC (highest deposition temperature applied) the film consists only of polycrystalline SnO_2. This behaviour is clearly illustrated in Fig. 1.

The grain size of the SnO_2 crystallites evaluated using Scherrer's equation increases with the oxygen pressure, whereas they decrease with the temperature raise. Fig. 2 shows the dependence of the grain size as a function of the substrate temperature at $P(O_2)$ = 20 Pa. As is seen the smallest grain size obtained is 90 nm for the film grown at 500 ^oC. The lattice constants of this film were calculated to be $\boldsymbol{a}$ = 0.473 nm and $\boldsymbol{c}$ = 0.317 nm, respectively, which are very close to those of the tetragonal SnO_2 ($\boldsymbol{a}$ = 0.475 nm and $\boldsymbol{c}$ = 0.319 nm) [35].

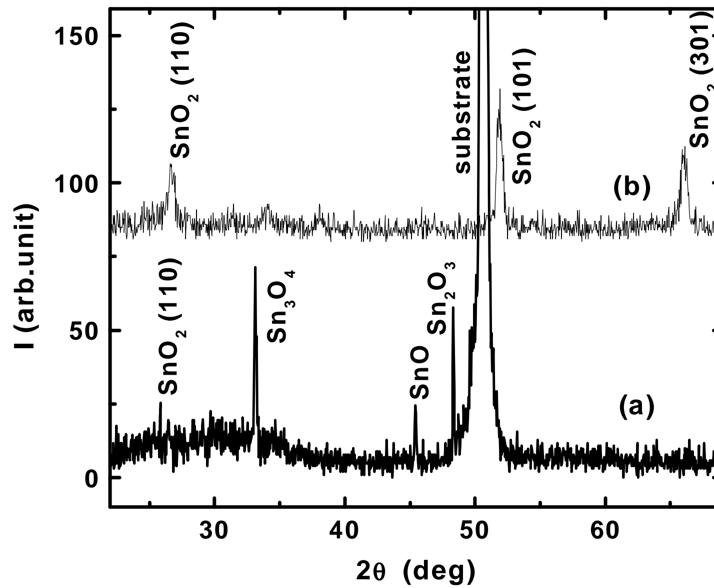

Fig. 1. XRD patterns of the films grown at 20 Pa oxygen pressure and substrate temperature: (a) 200 °C and (b) 500 °C.

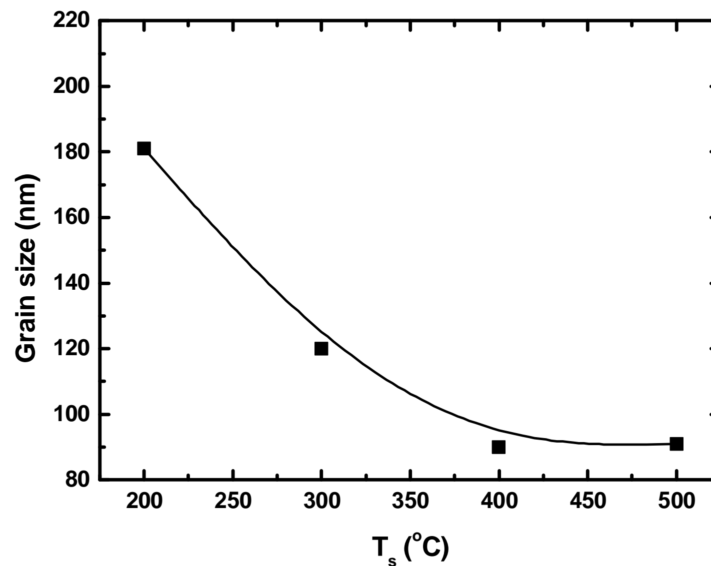

Fig. 2. Grain size of the films grown at 20 Pa as a function of substrate temperature.

The optical properties of the films are consistent with the structural ones. Fig. 3 shows the transmission spectra of the films deposited at different pressures. As is seen the layer grown at 20 Pa (Fig. 3 c) has maximum transmission value of 89 % at 940 nm. The optical band gap (***Eg***) was calculated from the optical transmission spectra using following relation $\boldsymbol{Eg} = 1241.5 / \lambda_c$ [34], where λ_c is the critical wavelength defined as the inflection point of the UV absorption edge. λ_c was determined from the second derivative of the transmission curve.

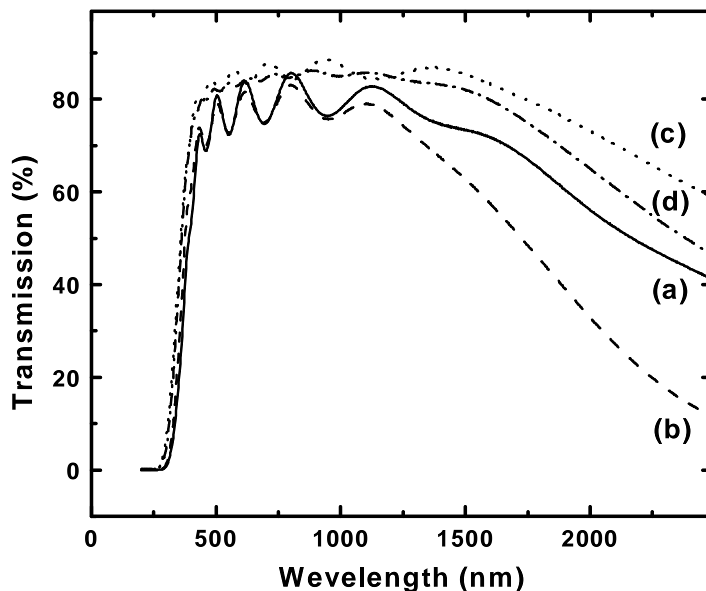

Fig. 3. Optical transmission spectra of the films grown at 200 °C and at different oxygen pressure: (a) 5 Pa; (b) 10 Pa; (c) 20 Pa and (d) 30 Pa.

Fig. 4 presents average optical transmission ***Ta*** evaluated as a mean value between the maximums and the minimums of the transmission spectra in the wavelength interval between 400 and 700 nm, and ***Eg*** as a function of oxygen pressure for the films deposited at 200 °C. As is seen, ***Eg*** has a constant value for the films grown at pressures up to 20 Pa and then significantly increases (from 3.37 to 3.99 eV) with further increase of the oxygen pressure. Moreover, ***Ta*** does not initially change when oxygen pressure rises. However, it increases slowly starting from 10 Pa and reaches a maximum value of 83 % at 20 Pa. Then it slightly drops with further pressure increase.

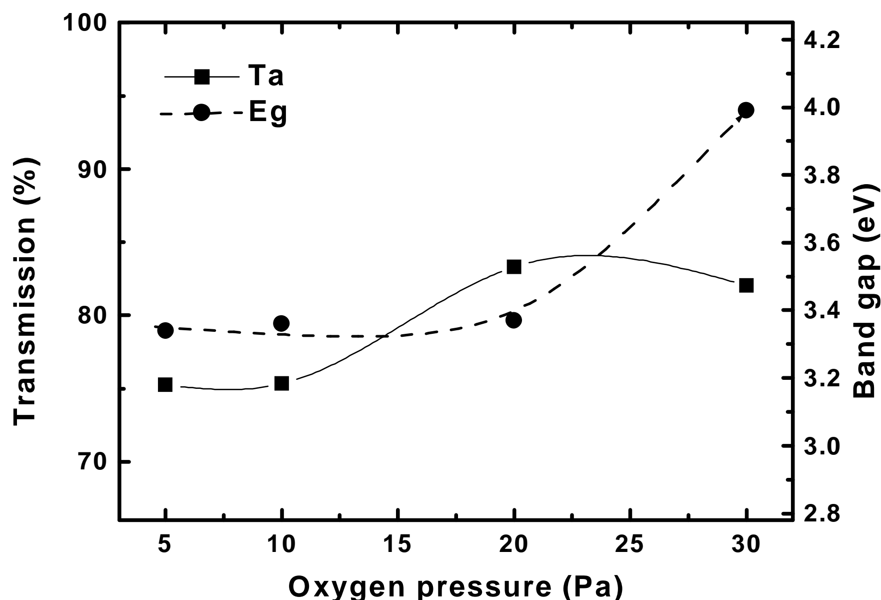

Fig. 4. Optical transmittance ***Ta*** in the visible region and band gap ***Eg*** as function of the oxygen pressure for the films grown at 200 °C.

This behaviour can be explained by the modification of the amount of oxygen vacancies with the oxygen pressure applied, which will modify the free carrier density and subsequently the absorbed energy. As a result, this will cause a shift of the absorption edge.

It was also found that the substrate temperature also affects on the optical properties of the tin oxide films. Fig. 5 represents the optical band-gap as function of the substrate temperature for the films deposited at $P(O_2)$ = 20 Pa. Additionally, some data taken from Ref. 36 are added for comparison. As is seen, there is a good coincidence between both experimental data.

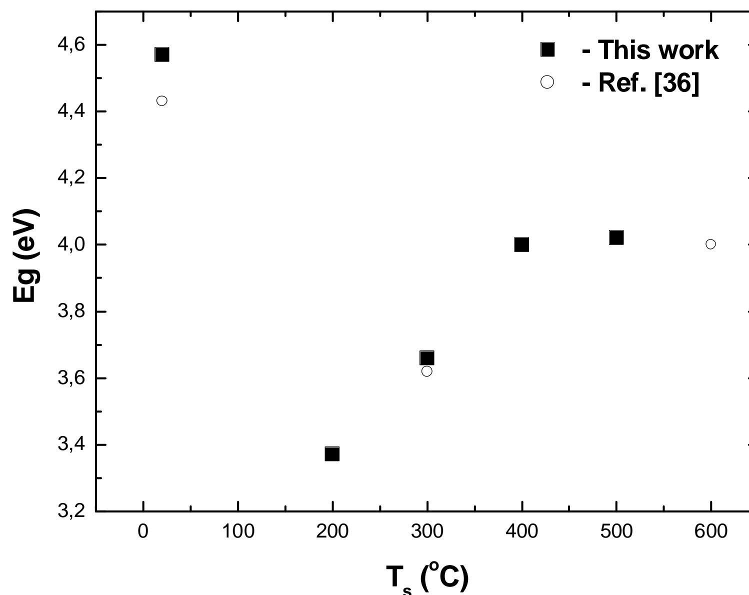

Fig. 5. Optical band gap of films grown at 20 Pa oxygen pressure for different temperature.

The lowest optical waveguide loss measured for the film grown at $P(O_2)$ = 20 Pa and T_s = 400 °C is 7 dBcm^{-1}. The thickness of the films depending on the growth conditions is between 200 nm and 400 nm. The measured refractive index of the layers is between 1.91 and 1.93. The films grown at 500 °C substrate temperature and 20 Pa oxygen pressure possess nearest value (1.93) to that of the bulk material (***n*** = 1.96) [35]. This confirms XRD results presented before, indicating that this film has the best crystalline properties.

4. Conclusion

The structural and optical analyses of the tin oxide films demonstrate that oxygen pressure and substrate temperature are very important parameters determining film quality. 20 Pa was found to be the optimal oxygen pressure for obtaining of thin tin oxide films with best structural and optical properties. The highest transmission of 89% in the visible region was observed for the film grown at 200 °C substrate temperature. The lowest optical waveguide loss measured is 7 dB.cm^{-1}. The best crystalline structure without any oxygen deficient phases has film grown at 500 °C, whose refractive index (***n*** = 1.93) was found to be the closest one to this of the bulk material.

The application of the films as optical gas sensors will be the subject of future investigation.

Acknowledgements

This work was supported in part by EU project NANOPHOS, Contract IST-2001-39112.

References

[1] A. Chowdhuri, P. Sharma, V. Gupta, J. Appl. Phys. **92**, 2172 (2002).
[2] J. H. Sung, Y. S. Lee, J. W. Lim, Sensors and Actuators B **66**, 149 (2000).
[3] C. K. Kim, S. M. Choi, I. H. Noh, Sensors and Actuators B **77**, 463 (2001).
[4] Y. Ozaki, S. Suzuki, M. Morimitsu, Sensors and Actuators B **62**, 220 (2000).
[5] W. Gopel, K. D. Schierbaum, Sensors and Actuators B **27**, 1 (1995).
[6] T. W. Kim, D. U. Lee, D. C. Choo, J. Appl. Phys. **90**, 175 (2001).
[7] J. R. Yu, G. Z. Huang, Y. J. Yang, Sensors and Actuators B **66**, 286 (2000).
[8] Z. Tang, G. Jiang, S. S. Lau, Sensors and Actuators B **43**, 161 (1997).
[9] Z. Tang, P. C. H. Chan, R. K. Sharma, Sensors and Actuators B **79**, 39 (2001).
[10] I. Sayago, J. Gutierrez, L. Ares, Sensors and Actuators B **27**, 19 (1995).
[11] G. Williams, G. S. V. Coles, Sensors and Actuators B **16**, 349 (1993).
[12] V. Lantto, J. Mizsei, Sensors and Actuators B **5**, 21 (1991).
[13] J. Klober, M. Ludwig, H. A. Sshneider, Sensors and Actuators B **3**, 68 (1991).
[14] G. G. Mandayo, E. Costano, F. J. Gracia, Sensors and Actuators B **95**, 90 (2003).
[15] H. Ogawa, M. Nishikawa, A. Abe, J. Appl. Phys. **53**, 4448 (1982).
[16] V. R. Katti, A. K. Debnath, K. P. Muthe, Sensors and Actuators B **96**, 245 (2003).
[17] B. K. Min, S. D. Choi, Sensors and Actuators B **98**, 239 (2004).
[18] C. D. Natale, F. Davide, G. Faglia, Sensors and Actuators B **23**, 187 (1995).
[19] P. Camagni, G. Faglia, P. Galinetto, Sensors and Actuators B **31**, 99 (1996).
[20] E. Comini, G. Faglia, G. Sberveglieri, Sensors and Actuators B **3953**, 1 (2001).
[21] G. Korotcenkov, V. Brinzari, Materials Science and Engineering C**19**, 73 (2002).
[22] C. Alfonso, A. Charai, J. Appl. Phys. **68**, 1207 (1996).
[23] S. Shukla, S. Patil, S. C. Kuiry, Sensors and Actuators B **96**, 343 (2003).
[24] D. Kotsikau, M. Ivanovskaya, D. Orlik, Sensors and Actuators B **101**, 199 (2004).
[25] G. Zhang, M. Liu, Sensors and Actuators B **69**, 144 (2000).
[26] G. Korotcenkov, V. Brinzari, Y. Blinov, Sensors and Actuators B **98**, 41 (2004).
[27] G. Korotcenkov, V. Macsanov, V. Brinzari, Sensors and Actuators B **96**, 602 (2003).
[28] J. H. Sung, Y. S. Lee, J. W. Lim, Sensors and Actuators B **66**, 149 (2000).
[29] C. Xu, J. Tamaki, N. Miura, Sensors and Actuators B **3**, 147 (1991).
[30] G. Sberveglieri, Sensors and Actuators B **6**, 239 (1992).
[31] C. K. Kim, S. M. Choi, I. H. Noh, Sensors and Actuators B **77**, 463 (2001).
[32] Y. Suda, H. Kawasaki, K. Doi, Surface and Coating Technology **175**, 1293 (2003).
[33] R. Dolbec, M. A. Khakani, A. M. Serventi, Sensors and Actuators B **93**, 566 (2003).
[34] R. Dolbec, M. A. Khakani, A. M. Serventi, Thin Solid Films **419**, 230 (2002).
[35] J. D. H. Donnay, Crystal data determinative tables, printed in USA, Washington (1963).
[36] S. Shanthi, C. Subramanian, P. Ramasamy, Cryst. Res. Technol. **34**, 1037 (1999).